scientific reports

Check for updates

OPEN

Frozen no more, a case study of Arctic permafrost impacts of oil and gas withdrawal

Kimberley Miner[1]✉, Latha Baskaran[1], Bradley Gay[1], Daniel Sousa[2] & Charles Miller[1]

Approximately 8100 km^2 of Alaska are leased to the oil and gas industry for exploration and extraction. According to industry estimates, subsurface expansion from these leases could cover up to 130.2 km^2 per pad. As industrial oil extraction activities increase across the thawing Alaskan permafrost, impacts on the permafrost environment will include rapid thaw, increased hydrological flux, and the release of climate warming greenhouse gases. Here, we use remote sensing and field observations to provide a first-order comparison of the direct impacts to the permafrost tundra from oil well pads, and the long-term consequences of a legacy oil pads on the warming North Slope of Alaska. We find that oil well pads on the permafrost accelerate permafrost degradation and persist despite remediation.

In 1986, Chevron and British Petroleum built the first and only oil well in the Arctic National Wildlife Refuge. A 700 m x 350 m pad supported a well called KIC-1 to which all infrastructure was transported over newly built roads from Kaktovik 15 miles to the southeast (Fig. 1)[1,2]. KIC-1 drilling reached a depth of 9631 m, but it is unknown if oil was discovered[3,4]. Soon after, the project stopped, the equipment on the site was disassembled, and the well was capped[4]. In the following years, remediation was completed to industry standards, the only known oil pad remediated on the Alaskan permafrost tundra[5]. Although there was no activity at KIC-1 in the 40 years since remediation, permafrost subsidence, pooling water, and areas of abrupt thaw are still visible, expanding past the region where the surface pad was initially established. As the KIC-1 site is undisturbed since remediation, it presents a unique case study for observing oil and gas pad impacts to the permafrost over time.

Since the development and remediation of the KIC-1 oil well, oil and gas exploration and withdrawal in the Alaskan North Slope are ongoing[6,7]. To date, almost 8,094 km^2 of Alaska are leased to the oil and gas industry for active withdrawal, in addition to the National Petroleum Reserve, which covers an additional 93,078 km^2 of permafrost tundra above the Arctic Circle[2,8]. Located inside the Arctic circle, Prudhoe Bay Oil Field in the North Slope is the United States' largest oil field, covering an area of 864.2 km^2 of permafrost tundra[1]. It was established in 1968, began production in 1977, and currently produces over 19,013 barrels of crude oil per day (~ 1.590 × 107 t/a)[1]. According to estimates from the oil industry, subsurface expansion from active oil and gas withdrawal could cover between 2 and 130.2 km^2 per pad, resulting in substantial below-ground permafrost disturbance[8].

Studies of the direct impacts on the permafrost landscape from oil pads have discovered that infrastructure development leads to changes to the movement of wildlife[9,10], increased permafrost thaw rates and water pooling[6,11,12], and pollution from anthropogenic refuse or aerosols[13–16]. Secondary impacts may include increased water flow and thermal impacts that create a marsh-like surface cover[6,17–19], and the release of organic carbon, microbes, and greenhouse gases[20–23]. Localized thaw can also introduce risks to critical infrastructure, including roads and airports[15,24,25]. While these studies have sought to understand the long-term ecosystem impacts to the permafrost from oil drilling[6,13,14,26–30], our effort to compare the residual impacts from a remediated legacy pad to the direct impacts of current infrastructure is a new application of cross-scale observational techniques.

While many of the direct, short-term impacts from oil well pads on the permafrost are known[1,6,7,12,31], the effort to couple these data with a characterization of long-term impacts from a remediated pad has not been completed. To further inform modeling and remote sensing efforts and understand the impacts occurring within a 100 m radius immediately surrounding oil well pads, we sampled four gravel pads along the Dalton Highway near Prudhoe Bay used for industrial purposes other than oil extraction (Fig. 1). Access to active oil wells and their surrounding pads is prohibited for security reasons. The 'proxy' pads are constructed in the same manner as the larger oil well pads and with similar, if not identical fill materials[6,8,25]. Then, to compare the direct impacts of pad development and the long-term impacts of remediated oil well pads, we utilized airborne imaging spectroscopy (hyperspectral imaging) to characterize ongoing permafrost effects from the remediated KIC-1 pad. This presents a novel opportunity to compare longer-term infrastructure effects with short-term, direct impacts from active pads, covering timescales ranging from daily to decadal. Our comparison of both

[1]NASA Jet Propulsion Laboratory, California Institute of Technology, Pasadena, USA. [2]Department of Geography, California State University at San Diego, San Diego, USA. ✉email: Kimberley.n.miner@jpl.nasa.gov

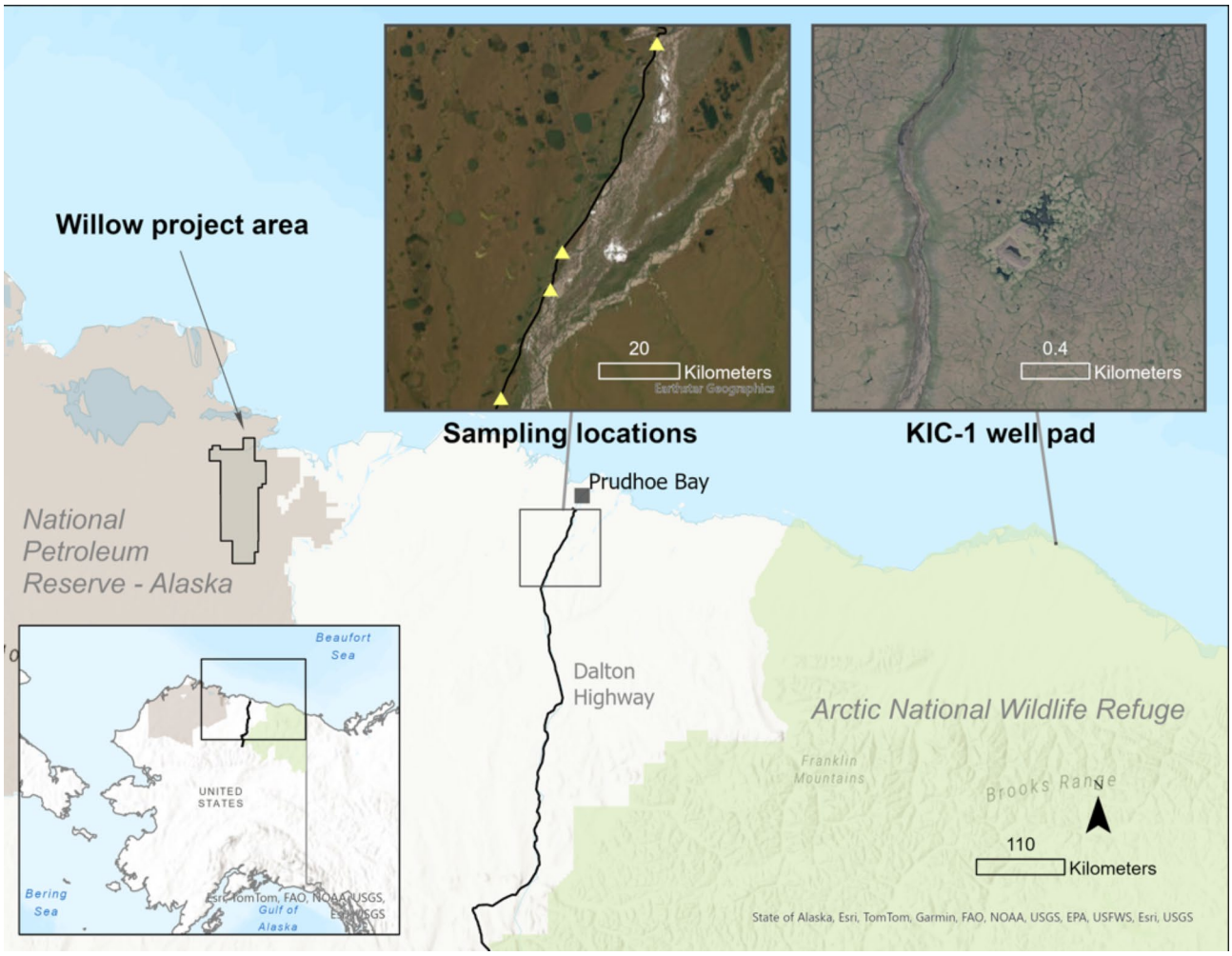

Fig. 1. Map of sampling locations from this paper, the remediated KIC-1 pad and the proposed Willow Project development area. Credit for background image of sampling location is Esri, Maxar, Earthstar Geographics, and the GIS User Community. Credit for the background imagery of KIC-1 is Maxar Products, Dynamic Mosaic © 2020 Maxar Technologies Inc., Alaska Geospatial Office, USGS. Figure was prepared using ArcGIS Pro 3.1.0 Copyright © 2023 Esri Inc. https://www.esri.com/en-us/arcgis/products/arcgis-pro/resources.

active and legacy oil well pads create a timeline from active pad use to post-remediation, outlining the primary and secondary effects of oil and gas infrastructure on the permafrost tundra.

Results

Direct measurements of pad impacts on the tundra

To understand the ongoing impact from gravel pads on the permafrost tundra of the Alaskan North Slope, samples were taken during July of 2023 over a series of days at both 5 cm and 15 cm depth in an area surrounding four industrial use gravel pads, to augment previous measurements[6,12,30,30,31]. Numerous physical relationships between the pads and the surrounding permafrost environment were identified as significant after Pearson Correlation Coefficient testing and corresponding significance testing. Further details are provided in the methods and supplementary sections.

Industrial and oil well pads on the permafrost tundra in Alaska are constructed from non-local gravel, introducing a novel substrate to the ecosystem[6,7,32]. This frequently used, cost-efficient strategy has a secondary consequence of amplifying warming, drying the local permafrost environment and driving pH changes[6,12,33]. For example, in our case study the elevated soil temperature and pH values decreased with distance from the pad, finally returning to background levels at approximately 60 m from the pads (Fig. 2, S1a,b).

The largest statistically significant correlations between physical relationships between the pad and the surrounding permafrost environment were found between soil moisture and soil temperature (0.266) and soil temperature and distance from pad (-0.481). This suggests that the addition of a pad changes the heat profile and increases the temperature of the surrounding environment and corroborates what is known from the literature (Fig. 2)[6,30]. Soil moisture and distance from pad (0.258) was also correlated, but was a less linear relationship due to the highly variable terrain, bordering on herbaceous wetland, and a proliferation of thermokarst lakes[6,13,30].

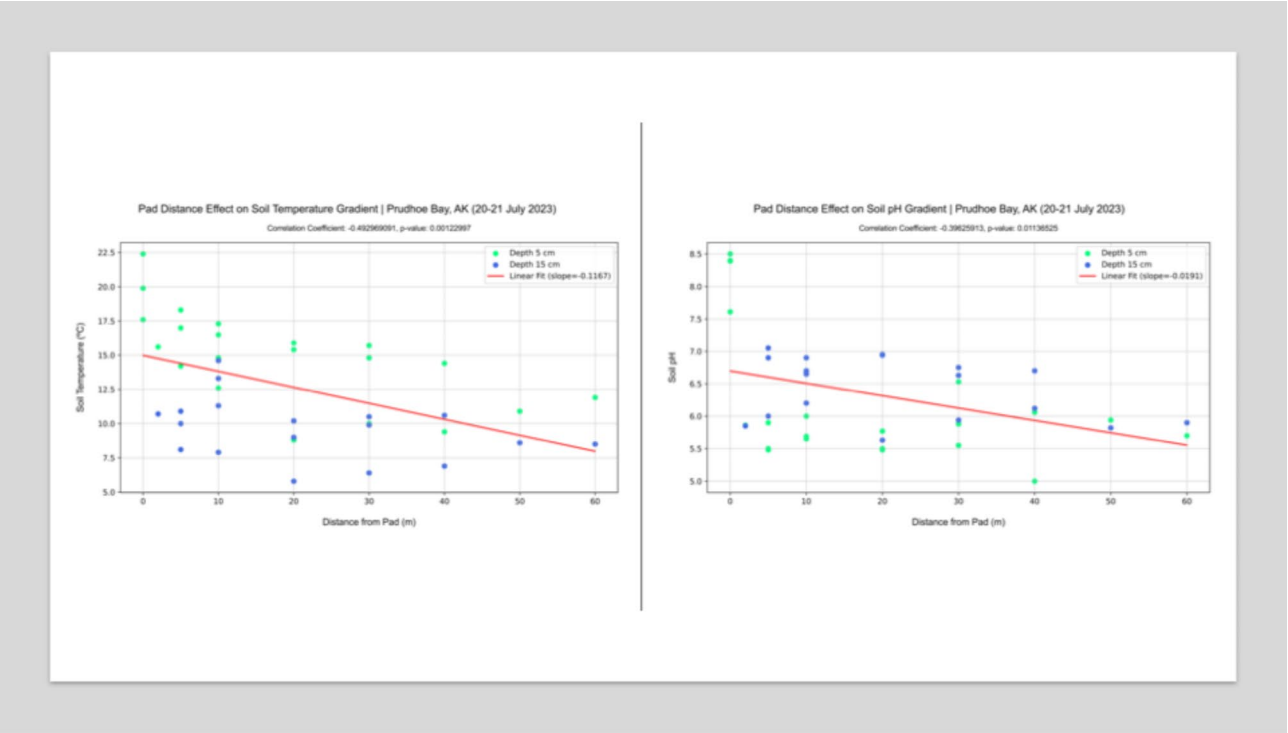

Fig. 2. Soil temperature and pH data from sampled locations along the Dalton Highway illustrating the stabilizing temperature, soil moisture and pH gradients at 5 cm and 15 cm depth, and increased distance from pad. The full dataset is available in the supplementary information.

We also found anticorrelated relationships between soil moisture and depth (-0.588), and soil temperature and depth (-0.692), the latter indicating the greatest statistical relationship and largest magnitude of negative correlation [= -0.6919, p-value 2.20327657E-36]. This is expected as the deeper measurements at 15 cm were often below the active layer, at the permafrost interface.

The relationship between soil pH and moisture (-0.662) is a known physical relationship[11,33], and demonstrated the largest negative ranking by magnitude according to the Spearman rank coefficient [= -0.7490, p-value 2.83555057E-03]. Soil pH and distance from pad (-0.400), soil pH and temperature (0.163), and soil pH and depth of soil profile measurement (0.142) were all correlated, illustrating known relationships[11,19,33,34], and another example of the potential impacts from the pad substrate[6,12,31]. While these measurements are a small subsample during an abbreviated period, they are in alignment with the body of literature[6,7,10,12] and emphasize that gravel pads directly impact permafrost state and condition.

Remote sensing analysis of pad remediation

While the ongoing impacts from gravel pads on the tundra provide critical data, the legacy of KIC-1, the only remediated oil well pad in the North Slope of Alaska, provides critical information about the long-term effects of gravel pads on the tundra. The footprint of the KIC-1 well pad is clearly visible in August 2022 true color AVIRIS-NG imagery (Fig. 3a, top left) despite being 40 years post remediation. Photogrammetry of the area makes visible extensive permafrost loss and subsidence at and surrounding the oil well pad[10]. Airborne imaging spectroscopy from NASA's Airborne Visible / Infrared Imaging Spectrometer—Next Generation (AVIRIS-NG)[35] shows vegetation changes and expanded polygonal hydrology from thawing permafrost. SWIR/NIR/Green (2250 nm, 850 nm, 550 nm) false color composite (Fig. 3a, top center) clearly captures variability in the KIC-1 pad site and non-photosynthetic vegetation in the surrounding tundra (magenta and red).

A linear spectral mixture model (Fig. 3a, top right; endmembers shown in bottom right) quantifies this variability. The maximum wavelength-explicit difference between mean spectra of the KIC-1 pad (Fig. 3a, lower left, N = 1500 pixels) and an equal number of pixels randomly sampled from nearby tundra (> 150 m from the nearest point on the KIC-1 well pad) was found to be 2.6% reflectance, less than 0.5 standard deviation of the spatial variability within the pad. The mean value of the wavelength-explicit difference spectra was 0.4% reflectance, with a standard deviation of 1.2%. These differences are so minor that they were not found to not be significantly different from 0 at the 90% level. Despite similarity in mean spectra, spatial variability in spectral signatures within KIC-1 is much more variable with two to four times greater standard deviation at all wavelengths (Fig. 3a, bottom center).

High-resolution optical imagery also demonstrates the impacts of KIC-1 on the permafrost tundra, illustrating the value of multiple remote sensing analysis to capture the impacts from infrastructure on remote and inaccessible regions. Native resolution (2 m ground sampling distance) true color WorldView-3 imagery

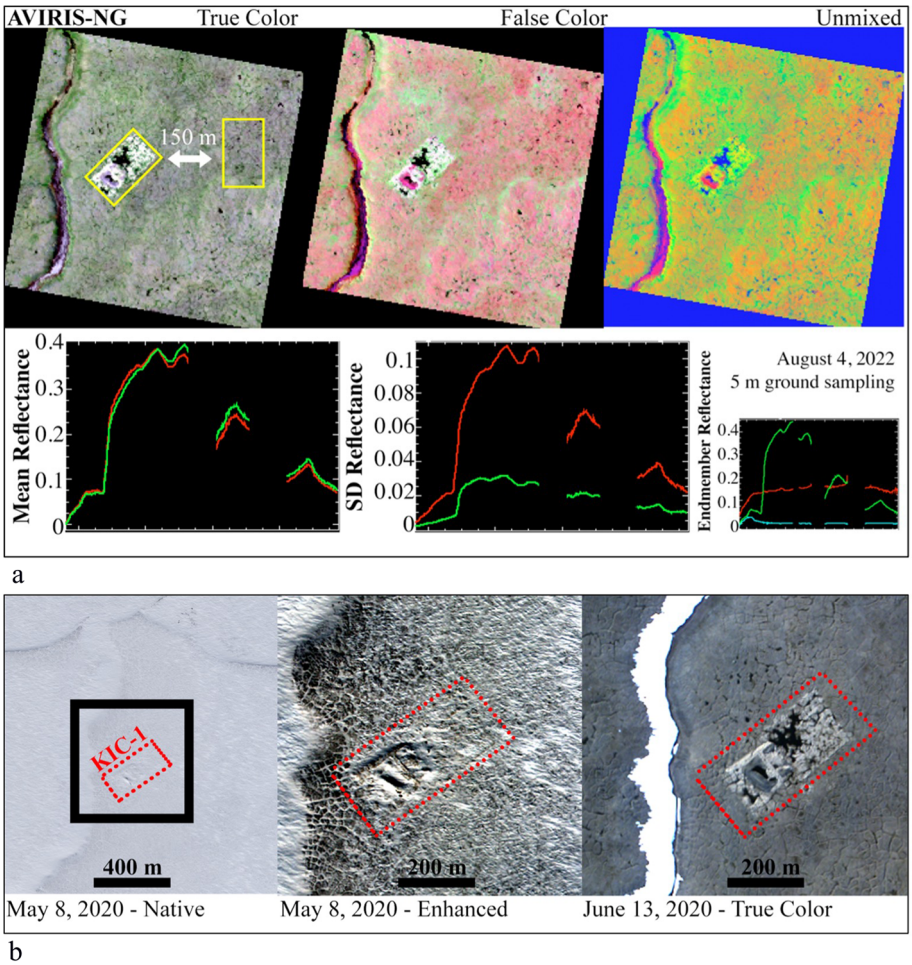

Fig. 3. **a** AVIRIS-NG Reflectance at KIC-1 acquired on August 4, 2022, show significant permafrost degradation within the original well pad borders and accelerated degradation in the adjacent tundra despite remediation best practices. Airborne imaging spectroscopy data were downloaded free-of-charge from the AVIRIS-NG data portal at: https://avirisng.jpl.nasa.gov/dataportal/. Figure were prepared using ENVI Classic Version 5.6: https://www.nv5geospatialsoftware.com/Products/ENVI. **b** Maxar imagery of the KIC-1 oil pads during summer 2020. Data were acquired through the NASA Commercial Smallsat Data Acquisition (CSDA) Program: https://www.earthdata.nasa.gov/esds/csda. ©2020 Maxar. Figure was prepared using ENVI Classic Version 5.6: https://www.nv5geospatialsoftware.com/Products/ENVI.

shows the north slope blanketed in late spring snow cover (Fig. 3b, Left image). The same image, enlarged and enhanced, shows the impacts of KIC-1 on snow pad accumulation and melt (Fig. 3b, center image). This image also highlights the significant polygonalization of the tundra immediately north and west of the KIC-1 oil well pad while the tundra to the east remains largely undisturbed. A true color WorldView-2 image captured approximately one month later in June 2020 shows extensive ponding and exposed substrate within the original well pad borders after snow melt (Fig. 3b, far right image). Imagery indicates that KIC-1 pad has had a lasting and observable impact on the tundra, even after remediation.

Discussion

Direct measurements of pad impacts on the tundra

The four proxy gravel pads along the Dalton highway utilized for this study encompass a proportionally smaller area than oil well pads. However, they have a similar structure and composition to both KIC-1 and active oil well pads, and they elevate infrastructure above the permafrost tundra with gravel. The pads sampled along the Dalton highway for this study are 2.3% smaller than the average oil well pad (0.02 km^2)[8]. The results from the surveyed sites are also representative of only aboveground activity, and they are not direct proxies for the larger active oil and gas pads. The operational oil and gas pads may have a substantially greater impact through heat flux, soil moisture, and pH changes both above and belowground, where they can disturb hundreds of acres of subsurface area per oil well pad[8].

All four study sites showed local warming and subsequent permafrost thaw extending away from the pad. Associated effects of this warming may include enhanced standing water and hydrological flow, surface warming, and permafrost thaw that expands from discrete pads into the surrounding environment (Figs. 2, 3)[36,37]. Further

examining the relationships between the pad and surrounding substrate, soil temperature decreases with distance from the pads, leading to a thermal gradient[6,12]. Additionally, the correlation between soil pH and the distance from well pads (-0.400) could suggest that warmer soils near well pad sites stimulate permafrost degradation and leaching from the pad. This localized warming can amplify subsurface thaw, contributing to an increase in water availability at depth. These relationships have been explored in the literature[6,7,12,13], and our smaller case study reiterates these findings.

Acidic pH is a common and critical characteristic of the permafrost soils of northern Alaska[33]. Permafrost soils contain considerable soil organic carbon, which can be up to thousands of years old[15,38], and could be released with permafrost thaw[37–39]. The pH buffering capacity of the permafrost soils is linked with water retention and coupled to carbon release[33], indicating that changes to the pH of the tundra, by itself, could have greenhouse gas emission potential.

Oil well pad gravel also has the potential to alter the delicate pH balance of surrounding permafrost[6].

As global temperatures increase, the deepening of the active layer causes permafrost to transition from stable, yearly freeze–thaw cycles to abrupt and punctuated thaw[40,41]. The localized temperature increases emanating from oil well pads exacerbate these dynamics by increasing water mobilization locally, with thaw expanding laterally[17,19]. Infrastructure accelerates thaw across the permafrost landscape, elevating the chances of greenhouse gas release and abrupt thaw[17,19,42]. The transition from a frozen environment to one of hydrologic flux changes the structure of the landscape[18,22,34,43], suggesting that subsequent remediation could be nearly impossible[44,45].

While our results are localized to the four case study proxy gravel pads, there are many similar pads and elevated roads in North Slope where ongoing soil profile measurements may provide further insights. These measurements could supplement the existing literature to map the subsurface dynamics that directly affect the evolution of above-ground permafrost topography and biodiversity.

Remote sensing analysis of pad remediation

Compared to the surrounding regions, the area around KIC-1 shows the persistence of disturbance effects. The well damage has expanded past the initial pad area, changing vegetation structure, deepening permafrost thaw, and increasing hydrologic intrusion into the collocated permafrost (Fig. 4). Looking at the Normalized Difference Vegetation Index (NDVI or greenness) and Normalized Difference Moisture Index (NDMI or wetness) shows that the vegetation surrounding KIC-1 has never recovered from the disturbance, with decreased vegetation growth under the footprint of the pad and extending out into the surrounding tundra. The NDMI

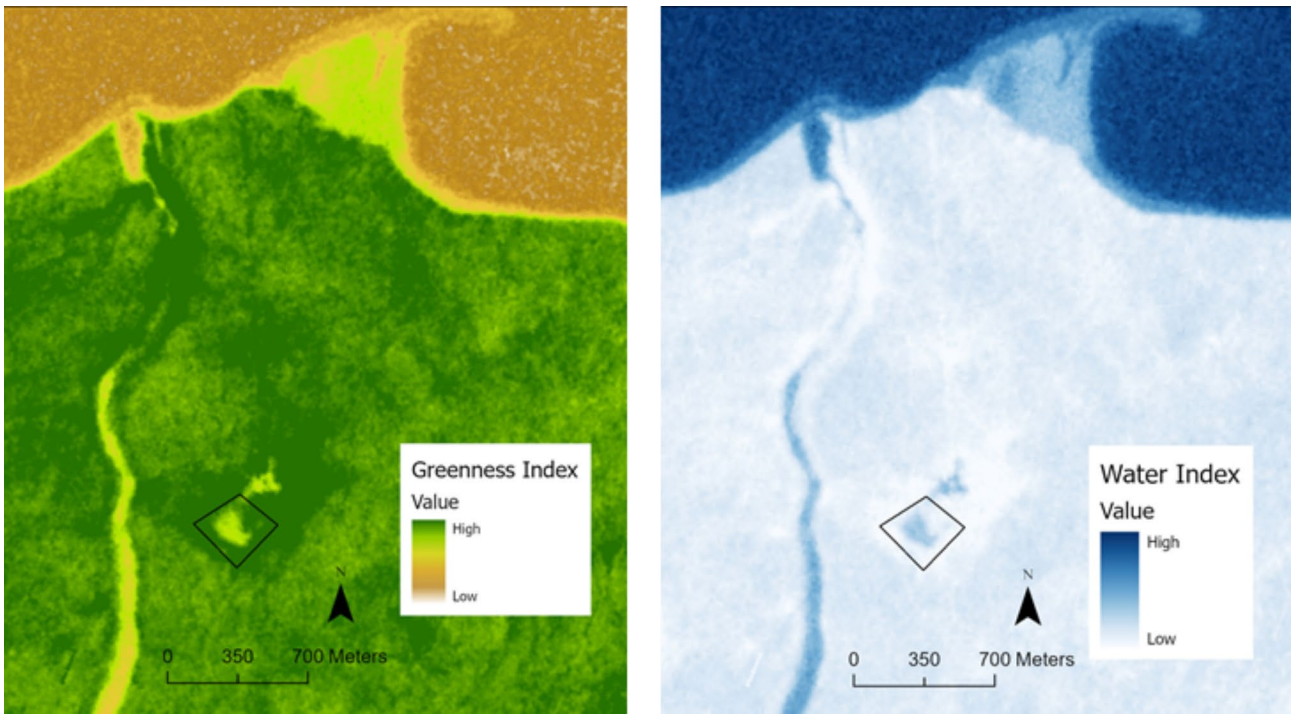

Fig. 4. Compiled greenness and water indices of KIC-1 from Planet Lab data acquired on August, 12 2020. Vegetation fraction shows progressive greening around the KIC well site, most prominent in late summer. Substrate fraction shows a progressive decrease in dry soils, presumably associated with increasing moisture due to permafrost thaw. Original data were acquired through the NASA Commercial Smallsat Data Acquisition (CSDA) Program: https://www.earthdata.nasa.gov/esds/csda. Image ©Planet Labs. Greenness and water indices were computed using ArcGIS Pro 3.1.0 Copyright © 2023 Esri Inc. Figure was prepared using ArcGIS Pro 3.1.0 Copyright © 2023 Esri Inc. https://www.esri.com/en-us/arcgis/products/arcgis-pro/resources.

of the permafrost within the region also shows considerably more moisture, indicating melted ice, permafrost thaw, and slumping (Fig. 4).

The KIC-1 oil well pad left an unmistakable impression on the landscape, where the underlying permafrost, tundra vegetation, water flow, and animal habitats are all altered. Future work should track the progression of in-use oil well pads, to develop a complete picture of permafrost impacts from oil and gas pads.

Future land cover change

Our study emphasizes that once permafrost degradation begins, it is difficult to remediate, and that the impacts of above-ground pads on the permafrost are considerable and lasting. However, the below-ground impacts to the subsurface environment may be substantially more extensive.

The National Petroleum Reserve in Alaska covers an area of 93,078 km^2 of permafrost tundra above the Arctic Circle. With the Willow project approved in 2023, further development is planned (Fig. 1)[46]. The Willow project will introduce an estimated 250 new oil well pads, each at ~ 40×50 ft^2.[46] To construct these pads, road, air, and water vehicles must bring infrastructure, supplies, and provisions, across over 405 km^2 of fragile permafrost tundra[46]. The Willow drilling project will last 30 years, ending its term in a considerably warmer world[47].

The Willow Project environmental impact report suggests substantial damage to critical fish stocks, polar bears, ungulates, raptors, walruses, seals, and numerous endangered whales caused by the construction and drilling[46]. The project would alter fragile habitat, changing the region's vegetative structure, range, and food system dynamics[4]. To fully understand the long-term impacts of construction for energy production on the Alaskan permafrost, further comprehensive studies must be accomplished. While remediation of the decommissioned oil well pads and infrastructure are offered as a solution, the long-term impacts of KIC-1 on the landscape illustrate that true remediation is not possible.

Next steps

Even a single oil well leaves an unmistakable scar on the landscape, changing the underlying permafrost, and the surrounding ecosystem. The current state of the KIC-1 oil well pad and surrounding area reiterates that the forecasted impacts of the Willow Project may be first order. Lasting effects may include extensive permafrost thaw, greenhouse gas release[41], hydrology and vegetation changes[17,45], the introduction of unknown microbes[15,48], ongoing pollution[13,14], and wildlife loss[2,9,10]. As international concern surrounding the Willow project grows, 40 years of KIC-1 oil well pad data show that the damage caused to the permafrost, tundra vegetation, and Arctic wildlife from drilling in the Alaska North Slope could be permanent, regardless of remediation.

Methodology

Spectral mixture analysis

Airborne imaging spectroscopy were analyzed and satellite-based multispectral imaging data were obtained using a linear spectral mixture analysis (SMA) framework, and applied to the AVIRIS-NG data (Fig. 3a)[49–51]. SMA is a simple, physically-based approach rooted in the observation that for most terrestrial systems, airborne and spaceborne optical imaging generates images with ground sampling distances coarser than the spatial scale of objects on the landscape[52]. Under conditions of linear mixing, the radiance (or reflectance) observed by each pixel can be considered an area-weighted average of the objects within its ground-projected instantaneous field of view (GIFOV). If these objects' radiance (or reflectance) spectra are known (or assumed), then their subpixel area contribution can be estimated. For the vast majority of terrestrial landscapes, most image variance can be explained as a linear combination of three spectral endmembers (EMs), corresponding to three common types of Earth materials: soil, non-photosynthetic vegetation, and rock Substrates (S), illuminated photosynthetic Vegetation (V), and Dark targets (D) like water or shadow[53–60,60]. We also examine the wavelength-explicit mixture residual[57]. (For more background on the application of spectral mixture analysis to spectral imagery, see[61]; for more background on the spectral properties and challenges of tundra landscapes, see[62–65]).

Spectral statistics

For equally-sized Regions of Interest (ROIs) around KIC-1 and undisturbed tundra, mean and standard deviation reflectance spectra were computed. Mean reflectance spectra for the KIC-1 pad ROI were visually compared to mean reflectance spectra for the ROI in the undisturbed tundra. ROI mean spectra were differenced and evaluated against the spatial dispersion in reflectance observed within each ROI. Both nonparametric and parametric statistical tests were used to evaluate spectral separability[55,58].

Maxar and planet data analysis

Maxar (WorldView-2 and WorldView-3) and Planet data were acquired from NASA via the Commercial Smallsat Data Analysis (CSDA) Program. Maxar images were obtained as netCDF files, converted to ENVI file format using *gdal_translate*, and orthorectified using ground control points provided with the image data. Planet data were ordered via the Planet API. Normalized Difference Vegetation Index (NDVI) [(NIR-Red)/(NIR + Red)] and Normalized Difference Water Index (NDWI) [(NIR-SWIR)/(NIR + SWIR)] were computed using image processing tools.

Direct measurement in the field

In July 2023, a small field team from NASA JPL sampled pads alongside the Dalton highway within 20 miles of Prudhoe Bay limits (Figs. 1, 5, S1a,b). Due to access challenges and security, four case study gravel pad sites with public access were selected adjacent to the Dalton Highway, representing smaller proxies for the oil well pads across the North Slope. These gravel pads are smaller than operational oil pads by a factor of 43.56[66]. All locations were built on gravel[32], elevated above the permafrost, at 90-degree angles to the Dalton Highway, and

Fig. 5. Sampling locations near Prudhoe Bay, AK, indicated by markers. The sample sites are along the Dalton Highway. The outset image shows the path of sampling at 90 degrees from the pad location. Background image of the sampling location provided by Esri, Maxar, Earthstar Geographics, and the GIS User Community. Figure was prepared using ArcGIS Pro 3.1.0 Copyright © 2023 Esri Inc. https://www.esri.com/en-us/arcgis/products/arcgis-pro/resources.

with minimal traffic at the site. Research was conducted by waling at a 90 degree angle from the pad, utilizing established field sampling methodologies (eg[37]). Three of the pads surveyed were used for pipeline maintenance, and one stored an above-ground generator enclosed in a metal, insulated shed. Researchers accessed the measurement sites by foot, endeavoring not to disturb areas near measurement locations.

Measurements of temperature, pH, soil moisture, wind speed and temperature were taken at 5 m intervals, at both 5 cm and 15 cm depths, using a Campbell Scientific HS2 | HydroSense II Handheld Soil Moisture Sensor (HS2, CS658, CS659) and Hanna Instruments Digital Soil Thermometer (HI45-01). Sites were sampled over two consecutive days in July to introduce minimal variance from weather and air temperature. *Full dataset in supplemental.*

Statistical analysis

We analyzed the biotic and abiotic covariates from the dataset to isolate site-level dynamics and drivers of change. We resolved outlier challenges in the dataset by implementing an interquartile function to isolate extreme values extending beyond two standard deviations of the mean, i.e., residing beyond the first (<0.05) and third (<0.95) quartiles of a normal distribution curve.

We evaluated and modified the dataframe distribution with stationarity tests (i.e., KPSS, ADF), trend differencing, serial correlation and *t*-derived multivariate co-integration testing (i.e., ACF, PACF, Johansen), and further constrained the dataset with interpolated dimensionality and multicollinearity reduction techniques. Multicollinearity reduction was facilitated by computing the Variance Inflation Factor (VIF) quotient and reducing the dataframe with subsequent feature engineering iterations, i.e., column removal. Applying this methodology (i.e., $VIF < 5$) into the preprocessing workflow reduces conditional hurdles and permits statistical analyses to be expedited.

We sorted the computed VIF values in descending order; however, the top two multicollinear candidates (e.g., 'Latitude', 'Site') were independent variables from the subsequent pre-processed dataset. Therefore, instead of removing this data, we reshaped the dataframe to accommodate a multi-index dataframe (i.e., 'Site', 'Latitude', 'Longitude') with five variables and specified attributes. After employment of dimensionality reduction and transformation features and covariates exhibiting the lowest p-values with highest and lowest correlation coefficients (r) by magnitude were assembled and reported (**S2**). *Additional data and figures are available in supplementary, all data is shared in a GitHub repository.*

Data availability

All data generated or analyzed during this study are included in this published article, its supplementary information files, or on GitHub https://github.com/bradleygay/wellpads

Received: 2 April 2024; Accepted: 11 October 2024
Published online: 25 October 2024

References

1. Szabo, D. J. & Meyers, K. O. Prudhoe Bay: Development History and Future Potential. in (OnePetro, 1993). https://doi.org/10.2118/26053-MS.
2. Arctic National Wildlife Refuge, 1002 Area, Petroleum Assessment, 1998, Including Economic Analysis. https://pubs.usgs.gov/fs/fs-0028-01/fs-0028-01.htm.
3. Fountain, H. Here's what oil drilling looks like in the Arctic Refuge, 30 Years Later. *The New York Times* (2017).
4. Mystery surrounds only oil well drilled in ANWR - Anchorage Daily News.
5. Jorgenson, M. T. & Jorgenson, J. C. Arctic Connections to Global Warming and Health. in *Climate Change and Global Public Health* (eds. Pinkerton, K. E. & Rom, W. N.) 91–110 (Springer International Publishing, Cham, 2021). https://doi.org/10.1007/978-3-030-54746-2_5.
6. Walker, D. A. et al. Cumulative impacts of a gravel road and climate change in an ice-wedge-polygon landscape, Prudhoe Bay, Alaska. *Arct. Sci.* **8**, 1040–1066 (2022).
7. Walker, D. A., Cate, D., Brown, J. & Racine, C. *Disturbance and Recovery of Arctic Alaskan Tundra Terrain* (1987).
8. Resource Development Council for Alaska, Inc. *Alaska's Oil and Gas Industry*. https://www.akrdc.org/oil-and-gas.
9. Johnson, H. E., Golden, T. S., Adams, L. G., Gustine, D. D. & Lenart, E. A. Caribou use of habitat near energy development in Arctic Alaska. *J. Wildl. Manag.* **84**, 401–412 (2020).
10. Raynolds, M. K. et al. Landscape impacts of 3D-seismic surveys in the Arctic National Wildlife Refuge, Alaska. *Ecol. Appl.* **30**, 1–20 (2020).
11. Abolt, C. J., Young, M. H., Atchley, A. L., Harp, D. R. & Coon, E. T. Feedbacks between surface deformation and permafrost degradation in ice wedge polygons, Arctic Coastal Plain, Alaska. *J. Geophys. Res. Earth Surf.* **125**, e2019JF005349 (2020).
12. Walker, D. A. et al. Cumulative impacts of oil fields on northern Alaskan Landscapes. *Science* **238**, 757–761 (1987).
13. Council, N. R. Cumulative environmental effects of oil and gas activities on Alaska's North Slope. *Cumul. Environ. Eff. Oil Gas Activ. Alaska's North Slope*https://doi.org/10.17226/10639 (2003).
14. Jones, N. Canada's oil sands spew massive amounts of unmonitored polluting gases. *Nature*https://doi.org/10.1038/d41586-024-00203-8 (2024).
15. Miner, K. R. et al. Emergent biogeochemical risks from Arctic permafrost degradation. *Nat. Climate Change* **11**, 809–819 (2021).
16. Kirillina, K., Shvetsov, E. G., Protopopova, V. V., Thiesmeyer, L. & Yan, W. Consideration of anthropogenic factors in boreal forest fire regime changes during rapid socio-economic development: Case study of forestry districts with increasing burnt area in the Sakha Republic, Russia. *Environ. Res. Lett.* **15** (2020).
17. Aas, K. S. et al. Thaw processes in ice-rich permafrost landscapes represented with laterally coupled tiles in a land surface model. *Cryosphere* **13**, 591–609 (2019).
18. Webb, E. E. et al. Permafrost thaw drives surface water decline across lake-rich regions of the Arctic. *Nat. Climate Change*https://doi.org/10.1038/s41558-022-01455-w (2022).
19. Andresen, C. G. et al. Soil moisture and hydrology projections of the permafrost region-a model intercomparison. *Cryosphere* **14**, 445–459 (2020).
20. Zhang, Z. et al. Emerging role of wetland methane emissions in driving 21st century climate change. *Proc. Natl. Acad. Sci. USA* **114**, 9647–9652 (2017).
21. Anthony, K. W. et al. 21St-century modeled permafrost carbon emissions accelerated by abrupt Thaw Beneath Lakes. *Nat. Commun.* **9**, 1–11 (2018).
22. Burke, S. A. et al. Long-term measurements of methane ebullition from thaw ponds. *J. Geophys. Res. Biogeosci.* **124**, 2208–2221 (2019).
23. Gross, M. Permafrost thaw releases problems. *Curr. Biol.* **29**, R39–R41 (2019).
24. Karjalainen, O. *et al.* Data descriptor: Circumpolar permafrost maps and geohazard indices for near-future infrastructure risk assessments. *Sci. Data* **6** (2019).
25. Melvin, A. M. et al. Climate change damages to Alaska public infrastructure and the economics of proactive adaptation. *Proc. Natl. Acad. Sci. USA* **114**, E122–E131 (2017).
26. Jorgenson, M. T. & Joyce, M. R. Six strategies for rehabilitating land disturbed by oil development in Arctic Alaska. *Arctic* **47**, 374–390 (1994).
27. Mobil, E. *Oil Spill Response Field Manual*. https://corporate.exxonmobil.com/-/media/global/files/risk-management-and-safety/oil-spill-response-field-manual_2014.pdf (2014).
28. Diversity, B. Arctic Ocean Drilling: Risking Oil Spills, Human Life, and Wildlife (2012).
29. de Gouw, J. A. et al. Daily satellite observations of methane from oil and gas production regions in the United States. *Sci. Rep.* **10**, 1–10 (2020).
30. Bergstedt, H. et al. The spatial and temporal influence of infrastructure and road dust on seasonal snowmelt, vegetation productivity, and early season surface water cover in the Prudhoe Bay Oilfield. *Arct. Sci.* **9**, 243–259 (2023).
31. Raynolds, M. K. et al. Cumulative geoecological effects of 62 years of infrastructure and climate change in ice-rich permafrost landscapes, Prudhoe Bay Oilfield, Alaska. *Glob. Change Biol.* **20**, 1211–1224 (2014).
32. Skorseth, K. & Selim, A. A. Gravel Roads: Maintenance and Design Manual.
33. Zheng, J., Berns-Herrboldt, E. C., Gu, B., Wullschleger, S. D. & Graham, D. E. Quantifying pH buffering capacity in acidic, organic-rich Arctic soils: Measurable proxies and implications for soil carbon degradation. *Geoderma* **424**, 116003 (2022).
34. Biskaborn, B. K. et al. Permafrost is warming at a global scale. *Nat. Commun.* **10**, 1–11 (2019).
35. Green, R. O. *et al.* Airborne Visible/Infrared Imaging Spectrometer 3 (AVIRIS-3). in 1–10 (IEEE, 2022).

36 Euskirchen, E. S., Bret-Harte, M. S., Scott, G. J., Edgar, C. & Shaver, G. R. Seasonal patterns of carbon dioxide and water fluxes in three representative tundra ecosystems in northern Alaska. *Ecosphere* **3**, art4 (2012).
37. Gay, B. A. et al. Investigating permafrost carbon dynamics in Alaska with artificial intelligence. *Environ. Res. Lett.* **18**, 125001 (2023).
38 Miner, K. R. et al. Permafrost carbon emissions in a changing Arctic. *Nat. Rev. Earth Environ.* **2022**(3), 55–67 (2022).
39. Jones, M. C. et al. Past permafrost dynamics can inform future permafrost carbon-climate feedbacks. *Commun. Earth Environ. Bold"*>*4*, 1–13 (2023).
40. Liu, Z. et al. Widespread deepening of the active layer in northern permafrost regions from 2003 to 2020. *Environ. Res. Lett.*https://doi.org/10.1088/1748-9326/ad0f73 (2023).
41. Turetsky, M. R. et al. Carbon release through abrupt permafrost thaw. *Nat. Geosci.* **13**, 138–143 (2020).
42. Bring, A. et al. Arctic terrestrial hydrology: A synthesis of processes, regional effects, and research challenges. *J. Geophys. Res. G Biogeosci.* **121**, 621–649 (2016).
43. Kurylyk, B. L., Hayashi, M., Quinton, W. L., McKenzie, J. M. & Voss, C. I. Influence of vertical and lateral heat transfer on permafrost thaw, peatland landscape transition, and groundwater flow. *Water Resour. Res.* **52**, 1286–1305 (2016).
44. Feng, J. et al. Warming-induced permafrost thaw exacerbates tundra soil carbon decomposition mediated by microbial community. *Microbiome* **8**, 3 (2020).
45. Heijmans, M. M. P. D. *et al.* Tundra vegetation change trajectories across permafrost environments and consequences for permafrost thaw. *Nat. Rev. Earth Environ.* **3** (2022).
46. BLM. Willow Master Development Plan Biological Assessment: Appendices (2022).
47. Rantanen, M. *et al.* The Arctic has warmed nearly four times faster than the globe since 1979. *Commun. Earth Environ.* **3** (2022).
48. Mackelprang, R. et al. Microbial survival strategies in ancient permafrost: Insights from metagenomics. *ISME J.* **11**, 2305–2318 (2017).
49. Adams, J. B., Smith, M. O. & Johnson, P. E. Spectral mixture modeling: A new analysis of rock and soil types at the Viking Lander 1 Site. *J. Geophys. Res. Solid Earth* **91**, 8098–8112 (1986).
50. Gillespie, A. *et al.* Interpretation of residual images: Spectral mixture analysis of AVIRIS images, Owens Valley, California. In: *Proceedings of Second Airborne Visible/Infrared Imaging Spectrometer (AVIRIS) workshop* 243–270 (NASA, Pasadena, California, 1990).
51. Smith, M. O., Ustin, S. L., Adams, J. B. & Gillespie, A. R. Vegetation in deserts: I. A regional measure of abundance from multispectral images. *Remote Sens. Environ.* **31**, 1–26 (1990).
52. Strahler, A. H., Woodcock, C. E. & Smith, J. A. On the nature of models in remote sensing. *Remote Sens. Environ.* **20**, 121–139 (1986).
53. Small, C. The Landsat ETM+ spectral mixing space. *Remote Sens. Environ.* **93**, 1–17 (2004).
54. Small, C. & Milesi, C. Multi-scale standardized spectral mixture models. *Remote Sens. Environ.* **136**, 442–454 (2013).
55. Small, C. & Sousa, D. Spectral characteristics of the dynamic world land cover classification. *Remote Sens.* **15** (2023).
56. Small, C. & Sousa, D. The Sentinel 2 MSI spectral mixing space. *Remote Sens.* (2022).
57. Sousa, D. *et al.* The spectral mixture residual: A source of low-variance information to enhance the explainability and accuracy of surface biology and geology retrievals. *J. Geophys. Res. Biogeosci.* **127**, e2021JG006672 (2022).
58. Sousa, D. & Small, C. Globally standardized MODIS spectral mixture models. *Remote Sens. Lett.* **10**, 1018–1027 (2019).
59. Sousa, D. & Small, C. Multisensor analysis of spectral dimensionality and soil diversity in the great Central Valley of California. *Sensors* **18**, 583 (2018).
60. Sousa, D. & Small, C. Global cross-calibration of Landsat spectral mixture models. *Remote Sens. Environ.* **192**, 139–149 (2017).
61. Adams, J. B. & Gillespie, A. R. *Remote Sensing of Landscapes with Spectral Images: A Physical Modeling Approach*. (Cambridge University Press, 2006).
62. Davidson, S. J. et al. Mapping Arctic tundra vegetation communities using field spectroscopy and multispectral satellite data in North Alaska, USA. *Remote Sens.* **8**, 978 (2016).
63. Liu, N., Budkewitsch, P. & Treitz, P. Examining spectral reflectance features related to Arctic percent vegetation cover: Implications for hyperspectral remote sensing of Arctic tundra. *Remote Sens. Environ.* **192**, 58–72 (2017).
64. Nelson, P. R. *et al.* Remote sensing of tundra ecosystems using high spectral resolution reflectance: opportunities and challenges. *J. Geophys. Res. Biogeosci.* **127**, e2021JG006697 (2022).
65. Thomson, E. R. et al. Multiscale mapping of plant functional groups and plant traits in the High Arctic using field spectroscopy, UAV imagery and Sentinel-2A data. *Environ. Res. Lett.* **16**, 055006 (2021).
66. Vehicle turnout length Guidance, State of Alaska.pdf

Acknowledgements

A portion of this work was done at the Jet Propulsion Laboratory, California Institute of Technology, under a contract with the National Aeronautics and Space Administration (80NM0018D0004). JPL is within the unceded land of the people known as the Tongva (Gabrielieño) within the limits of the Kizh Nation. D.S. gratefully acknowledges funding from the USDA NIFA Sustainable Agroecosystems Program (Grant #2022-67019-36397), the USDA AFRI Rapid Response to Extreme Weather Events Across Food and Agricultural Systems Program (Grant #2023-68016-40683), the NASA Land-Cover/Land Use Change Program (Grant #NNH21ZDA001N-LCLUC), the NASA Remote Sensing of Water Quality Program (Grant #80NSSC22K0907), the NASA Applications-Oriented Augmentations for Research and Analysis Program (Grant #80NSSC23K1460), the NASA Commercial Smallsat Data Analysis Program (Grant #80NSSC24K0052), the NASA FireSense Airborne Science Program (Grant #80NSSC24K0145), the California Climate Action Seed Award Program, and the NSF Signals in the Soil Program (Award #2226649).

Author contributions

KRM, LB, BAG, and DS completed the investigation, analysis, methodology development, and visualization for this text. KRM, LB, BAG, CEM and DS contributed to writing and revising the text.

Declarations

Competing interests

The authors declare no competing interests.

Additional information

Supplementary Information The online version contains supplementary material available at https://doi.org/10.1038/s41598-024-76292-2.

Correspondence and requests for materials should be addressed to K.M.

Reprints and permissions information is available at www.nature.com/reprints.

Publisher's note Springer Nature remains neutral with regard to jurisdictional claims in published maps and institutional affiliations.